

# Analytical Methods

Accepted Manuscript



This is an *Accepted Manuscript*, which has been through the Royal Society of Chemistry peer review process and has been accepted for publication.

*Accepted Manuscripts* are published online shortly after acceptance, before technical editing, formatting and proof reading. Using this free service, authors can make their results available to the community, in citable form, before we publish the edited article. We will replace this *Accepted Manuscript* with the edited and formatted *Advance Article* as soon as it is available.

You can find more information about *Accepted Manuscripts* in the [Information for Authors](#).

Please note that technical editing may introduce minor changes to the text and/or graphics, which may alter content. The journal's standard [Terms & Conditions](#) and the [Ethical guidelines](#) still apply. In no event shall the Royal Society of Chemistry be held responsible for any errors or omissions in this *Accepted Manuscript* or any consequences arising from the use of any information it contains.

## ARTICLE

# A label-free electrochemical impedance immunosensor for the sensitive detection of aflatoxin B<sub>1</sub>

Cite this: DOI: 10.1039/x0xx00000x

Received 00th January 2012,  
Accepted 00th January 2012

DOI: 10.1039/x0xx00000x

www.rsc.org/

Liguo Chen<sup>a,b</sup>, Jianhui Jiang<sup>a</sup>, Guoli Shen<sup>a</sup>, Ruqin Yu<sup>a\*</sup>

Because of the potential health impact of aflatoxin B<sub>1</sub> (AFB<sub>1</sub>), it is essential to monitor the level of this mycotoxin in a variety of foods and agricultural products. In this paper, a novel immunosensor for the rapid detection of AFB<sub>1</sub> based on label-free electrochemical impedance spectroscopy (EIS) monitoring was achieved. The immunosensor was fabricated by stepwise immobilization of 1, 6-hexanedithiol, colloidal Au, and aflatoxin B<sub>1</sub>-bovine serum albumin conjugate (AFB<sub>1</sub>-BSA) on a gold electrode via self-assembling technique. The interfacial properties of the modified electrodes were evaluated using Fe(CN)<sub>6</sub><sup>3-/4-</sup> redox couple as a probe via cyclic voltammetry (CV) and EIS. An equivalent circuit model with a constant phase element was used to interpret the obtained impedance spectra. The impedance via the specific immuno-interaction at the sensor surface was utilized to detect AFB<sub>1</sub> in samples. Under the optimized conditions, the impedance increment was linearly related to the AFB<sub>1</sub> concentration in the range of 0.08 and 100 ng mL<sup>-1</sup> with a detection limit of 0.05 ng mL<sup>-1</sup> (S/N = 3) and a correlation coefficient of 0.9919.

## 1 Introduction

The aflatoxins, primarily produced by *Aspergillus flavus* or *Aspergillus parasiticus*, are widely found in food crops including grains, cereals, peanut products, sorghum, and soy seeds<sup>1</sup>. In particular, aflatoxin B<sub>1</sub> (AFB<sub>1</sub>) (Figure 1), a commonly occurring toxin aflatoxin, is one of the most potent carcinogens with potential hazards to human and animal health<sup>2</sup>. Owing to the risk of aflatoxins, the current maximum tolerable levels for aflatoxins issued by the European Commission are 2 ng g<sup>-1</sup> for AFB<sub>1</sub> and 4 ng g<sup>-1</sup> for total aflatoxins (AFB<sub>1</sub>, AFB<sub>2</sub>, AFG<sub>1</sub> and AFG<sub>2</sub>) in corn, groundnuts, nuts, dried fruit and cereals<sup>3,4</sup>. For such a low content, developing simple, selective and sensitive analytical methods to detect the trace amount of AFB<sub>1</sub> in foodstuffs and feeds is an extremely important issue.

During the past two decades, various analytical techniques have attracted increasing attention to the determination of aflatoxins such as thin layer chromatography (TLC)<sup>5</sup>, gas chromatography coupled with mass spectrometry (GC/MS) and high-performance liquid chromatography (HPLC)<sup>6-11</sup>, capillary electrophoresis (CE)<sup>12</sup>, and a variety of immunoassay methods<sup>13-16</sup>. These methods are highly sensitive and specific, but are often complicated and time-consuming, or need some secondary antibodies, or rely on expensive instruments or skillful operators. For example, among the conventional immunoassay methods, the enzyme-linked

immunosorbent assays (ELISA)<sup>16</sup> is undoubtedly the most frequently applied one.

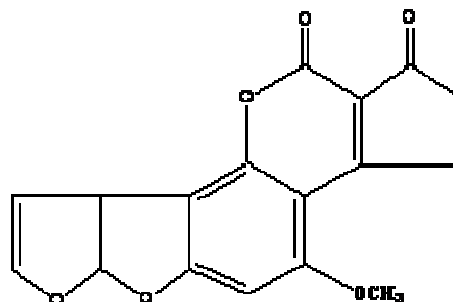


Figure 1. Chemical structure of AFB<sub>1</sub>

Nevertheless, there are some limitations of ELISA such as depending on some complicated enzyme labeling procedure and specific reagents of synthesized redox-labeled detection probes, consequently preventing its widespread use in common practice. Thus, there is an urgent demand for ultra sensitive methods of immunoassay. Label-free electrochemical immunosensors<sup>17-24</sup> can offer advantages over chromatographic procedures or ELISA. They have been reported to be a very attractive approach for detecting affinity interactions by monitoring changes of electronic or interfacial properties generated by the immunocomplex formation on the electrode surface. Sun et al.<sup>22</sup> described a simple, highly

sensitive, label-free, and mediatorless approach for fabrication of impedimetric immunosensor based on immobilization of anti-MCLR on gold electrode. Qiu et al.<sup>23</sup> designed a label-free amperometric immunosensor based on the chitosan-branched ferrocene and gold nanoparticles for detecting hepatitis B surface antigen. Radia and coworkers<sup>24</sup> prepared a novel label-free electrochemical impedimetric immunosensor for sensitive detection of ochratoxin A. It is widely accepted that the impedance sensing is a very good choice for biological binding events with fast, simple and the low-cost characteristics. However, This method has seldom been applied in detection of AFB<sub>1</sub> up to now.

The current work focused on development of a label-free impedimetric immunosensor to determine AFB<sub>1</sub> level. The results revealed that the sensitivity could be substantially improved via the self-assembled colloidal. Under the optimized conditions, there was a good linear relationship between impedance increment and the concentration of AFB<sub>1</sub> in the range of 0.08 and 100 ng mL<sup>-1</sup>. The detection limit can reach as low as 0.05 ng mL<sup>-1</sup>. Our method is a very promising alternative in the determination of AFB<sub>1</sub>.

## 2 Experimental sections

### 2.1 Chemicals

Aflatoxin B<sub>1</sub> (AFB<sub>1</sub>), Aflatoxin B<sub>2</sub> (AFB<sub>2</sub>), Aflatoxin M<sub>1</sub> (AFM<sub>1</sub>), Aflatoxin M<sub>2</sub> (AFM<sub>2</sub>), AFB<sub>1</sub>-bovine serum albumin (BSA) conjugate (AFB<sub>1</sub>-BSA) and the monoclonal anti-Aflatoxin B1 (from mouse) were provided by Sigma-Aldrich Co. (St. Louis, MO, USA). Bovine serum albumin (BSA) was provided by Beijing Zhongshan Golden Bridge Biotechnology Co., Ltd (Beijing, China). 1,6-Hexanedithiol was obtained from Fluka. H<sub>2</sub>SO<sub>4</sub> and trisodium citrate were obtained from Shanghai Chemical Reagents (Shanghai, China). The phosphate buffer solution (PBS) used was a 10 mmol L<sup>-1</sup> Na<sub>2</sub>HPO<sub>4</sub>-KH<sub>2</sub>PO<sub>4</sub> solution of pH 7.4. The K<sub>3</sub>[Fe(CN)<sub>6</sub>]/K<sub>4</sub>[Fe(CN)<sub>6</sub>] mixture solution (1:1, 5 mmol L<sup>-1</sup>) used in electrochemical measurements were prepared by using 10 mmol L<sup>-1</sup> PBS (containing 0.1 mol L<sup>-1</sup> KCl, pH 7.4). All other chemicals were of analytical grade and used as received. Doubly distilled water was used throughout all the experiments.

### 2.2 Apparatus

The instruments used for cyclic voltammetry (CV) and electrochemical impedance spectroscopy (EIS) measurements were carried out on a CHI 660a working station (CH Instruments, Shanghai, China) in conjunction with a computer. Throughout all the experiments, a three-electrode system was used, with a fabricated electrode (a gold disk electrode, 4 mm diameter) as a working electrode, a saturated calomel electrode (SCE) as a reference electrode and a platinum electrode as an auxiliary electrode. Impedance measurements were performed in the frequency range from 0.1 Hz to 10,000 Hz. All potentials were measured and reported versus the SCE, and all measurements were carried out in a 25-mL cell at room temperature.

### 2.3 Synthesis of Gold Nanoparticles

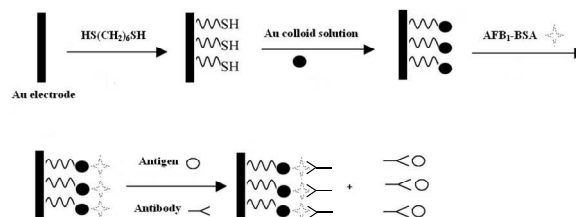
All glassware used for gold nanoparticle synthesis were thoroughly cleaned in freshly prepared aqua Regia (three parts of HCl plus one part of HNO<sub>3</sub>), followed by extensive rinsing with doubly distilled water. Gold nanoparticles were prepared according to the literature<sup>25</sup> with a slight modification. Briefly, 1 mL of 1.0% trisodium citrate was added into 100 mL of 0.01% HAuCl<sub>4</sub> the mixed solution was refluxed under stirring, and then the mixture was kept boiling for another 10 min. While the solution color turned to deep wine red, the heating continued for 15 minutes and the heater was removed. The

mixture was stirred continuously until it was cooled to room temperature. Colloidal Au solution thus prepared was stored in a brown glass bottle at 4 °C for use.

### 2.4 Fabrication of immunosensor and Measurement procedure

First, the gold electrode was polished with a 0.05 μm alumina powder and successively soaked into water, ethanol and water for 5 min each under ultrasonic agitation. Then, the gold electrode was dipped in "piranha" solution (H<sub>2</sub>SO<sub>4</sub>/H<sub>2</sub>O<sub>2</sub>, 7:3 by volume) (Warning: Piranha solution reacts violently with almost all organic materials and must be handled with extreme caution!) for 30 min and electrochemically treated by cycling the potential between -1.0 and +1.55 V in 0.1 mol L<sup>-1</sup> H<sub>2</sub>SO<sub>4</sub> for 10 min. After that, the electrode was washed with doubly distilled water and dried in a nitrogen stream at room temperature<sup>26</sup>. The prepared bare electrode was placed in a freshly made 2.5 mmol L<sup>-1</sup> 1,6-hexanedithiol solution in ethanol. After adsorption for 4 h, the electrode was thoroughly washed with ethanol and water to remove physically adsorbed 1,6-hexanedithiol and dried at room temperature. Subsequently, the electrode was immersed in the Au nanoparticle solution overnight in a refrigerator. After sufficiently rinsing, the electrode was incubated in an AFB<sub>1</sub>-BSA solution for 4 h at room temperature in order to adsorb enough immuno-antigen on the electrode, and then it was rinsed thoroughly with 10 mmol L<sup>-1</sup> PBS to remove the unstable AFB<sub>1</sub>-BSA on the electrode surface. To block the possible remaining active sites and avoid the non-specific adsorption on the electrode surface, the electrode was dipped in a 5.0% BSA solution for 30 min at room temperature. Finally, the immunosensor obtained was rinsed with water and PBS (pH 7.4) to remove the physically adsorbed molecules and stored in PBS at 4 °C when not in use.

For the measurement, antigen and antibody with different concentrations were dissolved in 10 mmol L<sup>-1</sup> PBS (pH 7.4). After 50 min incubation at 37 °C, the resulting electrode was washed with doubly distilled water and PBS, separately. The impedance changes of the immunosensors were measured in a solution of 5 mmol L<sup>-1</sup> K<sub>3</sub>[Fe(CN)<sub>6</sub>]/K<sub>4</sub>[Fe(CN)<sub>6</sub>] (1:1, containing 0.1 mol L<sup>-1</sup> KCl, pH 7.4) mixture solution. (Scheme 1)



**Scheme 1.** Schematic illustration of the process of immobilization of immunoantigen onto the gold electrode and the immunoreactions procedure

## 3 Results and discussion

### 3.1 Electrochemical characteristics of the modifying process

The electron-transfer behaviors for the AFB<sub>1</sub> immunosensor by self-assemble technique in preparation processes were performed by cyclic voltammetry. Figure 2 shows the typical CV of the fabricated AFB<sub>1</sub> immunosensor in the presence of 5 mmol L<sup>-1</sup> ferrocyanide/ferricyanide mixture (1:1) solution containing 10 mmol L<sup>-1</sup> PBS (pH 7.4) and 0.1 mol L<sup>-1</sup> KCl. As can be seen, Figure 2a depicts an intact pair of redox peaks for the CV of the bare Au electrode. The immobilization of 1,6-hexanedithiol on the gold electrode leads to a significant decrease in peak current of the redox

probe (Figure 2b). The formation of insulating film partially blocked the electron-transfer of  $[\text{Fe}(\text{CN})_6]^{3-/4-}$  to the modified electrode. When the Au nanoparticles were modified onto the electrode surface, a slight increase of the current response can be found in Figure 2c. It indicates that the Au nanoparticles can enhance the efficiency and rate of electron transfer at the electrode surface. As expected, the subsequent chemical binding of the AFB<sub>1</sub>-BSA induces an obvious reduce of current response in the electrochemical signal (Figure 2d), exhibiting that the immobilization of the AFB<sub>1</sub>-BSA builds up an almost insulating layer on the Au electrode and hinders the interfacial electron transfer.

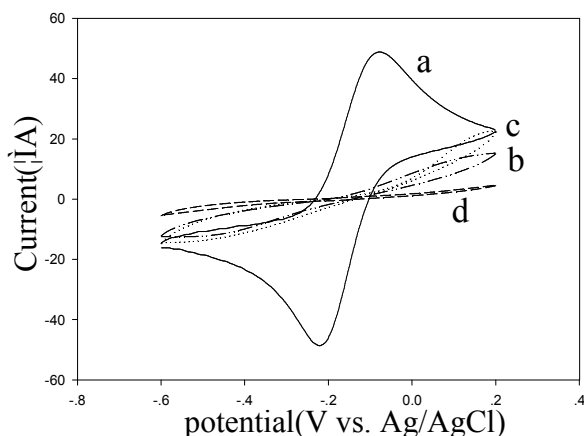
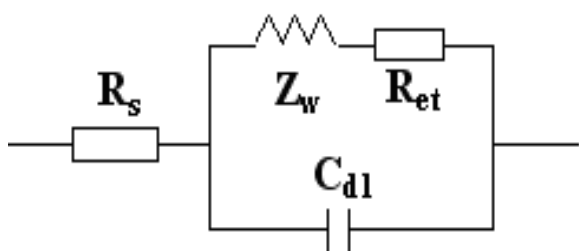


**Figure 2.** Cyclic voltammograms of 5mM  $\text{K}_4[\text{Fe}(\text{CN})_6]/\text{K}_3[\text{Fe}(\text{CN})_6]$  (1:1) in PBS (0.1M KCl, pH 7.4) after different steps of modification; (a) bare gold electrode; (b) 1,6 hexanedithiol/gold electrode; (c) Au-colloid/1,6 hexanedithiol/ gold electrode; (d) AFB<sub>1</sub>-BSA ( $10 \mu\text{g mL}^{-1}$ )immobilized gold electrode. Scan rate:  $100\text{mVs}^{-1}$ vs.SCE.

### 3.2 Electrochemical impedance characteristics of the modifying process

Electrochemical impedance spectroscopy is one of the most effective methods to investigate the interface features of surface-modified electrodes and has been extensively developed in the field of immunosensors<sup>27-29</sup>. A typical shape of a Faradic impedance spectroscopy usually includes a semicircle portion and a straight line one. The semicircle portion is found at higher frequencies corresponding to the electron transfer limiting process, and the linear portion is found at the low frequencies resulting from the diffusion limiting step of the electrochemical process, respectively. As shown in Scheme 2, the impedance spectroscopy was represented as an equivalent circuit<sup>30</sup>.



**Scheme 2.** Equivalent circuit to fit the impedance spectroscopy in the presence of redox couples:  $R_s$ , resistance of the electrolyte

solution;  $R_{et}$ , electron-transfer resistance;  $Z_w$ , Warburg impedance;  $C_{dl}$ , double-layer capacitance.

The equivalent circuit includes the ohmic resistance of the solution resistance ( $R_s$ ), the Warburg impedance element ( $Z_w$ ), the double layer capacitance ( $C_{dl}$ ) and the electron transfer resistance ( $R_{et}$ ). The two components,  $R_s$  and  $Z_w$ , represent bulk properties of the electrolyte solution and diffusion feature of redox probe in solution, respectively. Accordingly, these parameters are not affected by the electrochemical reaction occurring at the electrode surface.  $C_{dl}$  and  $R_{et}$  depend on the dielectric and insulating features at the electrode/electrolyte interface, respectively.

Figure 3 shows the electrochemical impedance spectroscopy for each step to reflect the procedure of the immunoassay. As shown in Figure 3, the Faradic impedance spectroscopy on a bare gold electrode reveals a straight line (curve 3a), implying that the electron-transfer process is not a limiting step of the electrochemical process. The Au-colloid/1,6-hexanedithiol/gold electrode, curve 3b, the semicircle diameter increases obviously indicating a lower electron-transfer resistance at the electrode interface. With the immunocomplex formation on the electrode (curves 3c and 3d), the semicircle diameter increases apparently compare with curve 3b, illustrates the AFB<sub>1</sub>-BSA and BSA film was successfully immobilized on the electrode surface. After immunoreactions results in a remarkably increase in the semicircle diameter of the impedance spectrum (curve 3e), implying the interfacial electron-transfer rate on electrode increases remarkably. The increase of diameter of the semicircle confirms that the immunoreactions were successfully completed on the electrode surface. When AFB<sub>1</sub> exists in solution, the concentration of free antibody decrease, which leads to the reduction of the antibody volume combined on AFB<sub>1</sub>-BSA surface and the corresponding electrochemical impedance of the immunosensor. All the impedance measurements were performed in the presence of a redox probe  $\text{K}_4[\text{Fe}(\text{CN})_6]/\text{K}_3[\text{Fe}(\text{CN})_6]$  at the scanning frequencies from 0.1 to 10 kHz.

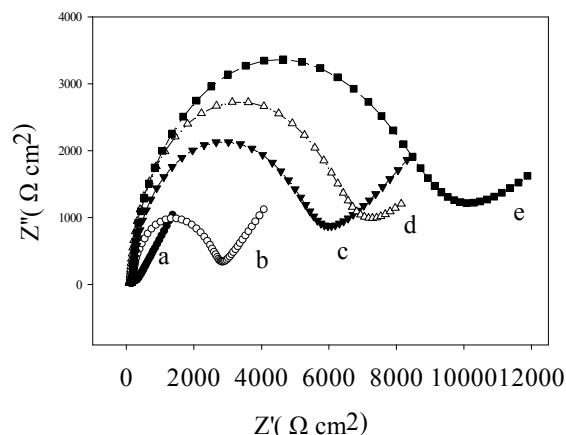


**Figure 3.** Nyquist diagram of electrochemical impedance spectroscopy for the immunosensor electrode at a potential +0.24 V vs. SCE: (a) Bare Au electrode; (b) Au-colloid/1,6-hexanedithiol/gold electrode; (c) AFB<sub>1</sub>-BSA immobilized electrode; (d) After immersed in BSA; (e) Resulting electrode after immunoreaction at 37 °C. All the measurements were carried out in 10 mM PBS (containing 0.1M KCl, 5 mM  $\text{K}_4[\text{Fe}(\text{CN})_6]/\text{K}_3[\text{Fe}(\text{CN})_6]$ , pH 7.4) and the data were recorded in the frequency range from 0.1 Hz to 10 kHz.

### 3.3 Optimization of the experimental conditions

#### 3.3.1 Influence of pH on the AFB<sub>1</sub>-BSA adsorption onto the colloidal Au-modified electrode

The configurations and electrostatic states of proteins usually depend on the medium pH, so that the pH value should be of great importance in the proteins immobilization process. Figure 4 shows the effects of pH of adsorbing AFB<sub>1</sub>-BSA onto the colloidal Au-modified electrode was tested over a pH range from 4.5 to 10.0. As manifested in Figure 4, an optimum relationship between the impedance change of the resulting electrode and the pH of the PBS was observed at around pH 7.4, which was used in all experiment.

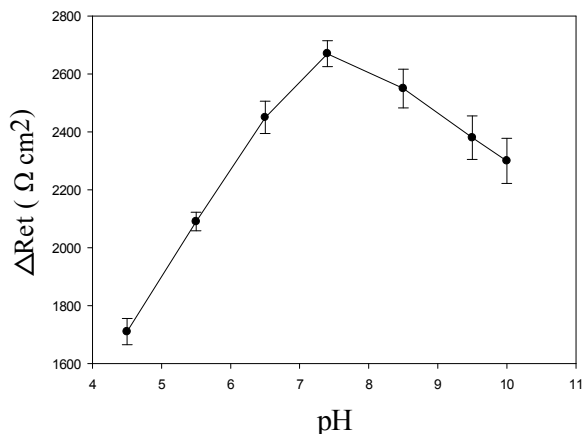


**Figure 4.** Effect of the pH for the immobilization of AFB<sub>1</sub>-BSA on the impedance change. For optimization, in the experiment, the AFB<sub>1</sub> antibody dilution ratio at 1:4000 and 0.5 ng mL<sup>-1</sup> AFB<sub>1</sub> was applied and the incubation time was 40 min (n=3, error bar represented R.S.D.).

### 3.3.2 Effect of incubation time on the antibody immobilization

As seen in Figure 5, the incubation time for immunoassay was investigated as a factor influencing the transducer performance. When incubation time was over 50 min, the impedance changes did not increase further, indicating that the immunoreaction on the electrode was almost completed. Therefore, the immunochemical incubation time of 50 min was selected to evaluate the analytical performance of the sensor in all the subsequent assays.

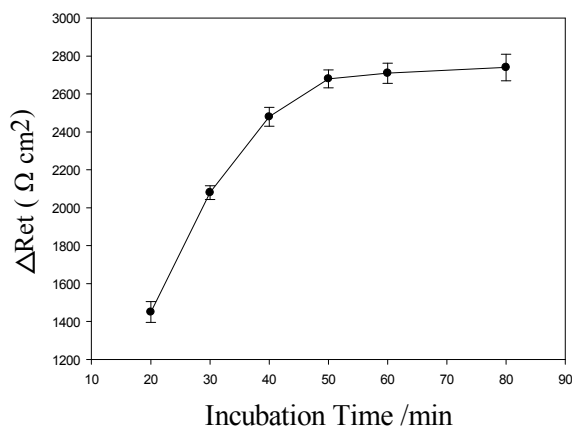


**Figure 5.** Effect of the incubation time of the immunoreaction on the resulting electrode. Incubation time from 20 min to 80 min. In this experiment, the AFB<sub>1</sub> antibody dilution ratio at 1:4000 and 0.5 ng mL<sup>-1</sup> AFB<sub>1</sub> was utilized (n=3, error bar represented R.S.D.).

### 3.3.3 Effect of the AFB<sub>1</sub> monoclonal antibody concentration

The effect of antibody concentration of the immunosensor in the immunoreaction was also investigated. The relation between the

impedance changes caused by the immunoreaction and the dilution ratio of antibodies was shown in Figure 6. One can observe that the impedance changes decrease with the AFB<sub>1</sub> monoclonal antibody titer up to 1:20000 and then decrease distinctly at higher dilution ratios. Because the number of adsorptive sites is limited, saturated binding of AFB<sub>1</sub> could be reached by increasing AFB<sub>1</sub> antibody titer. Higher titers of antibodies might presumably result in increased disorder in the alignment of adsorbed AFB<sub>1</sub> antibody and spatial hindrance of immunoreaction. Thus, the AFB<sub>1</sub> antibody concentration of 1:20000 titer was recommended for all the subsequent experiments.

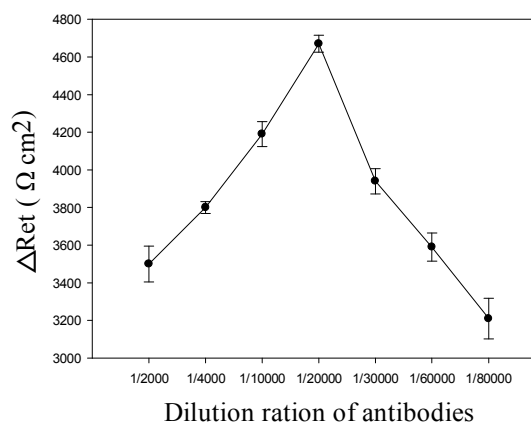


**Figure 6.** Relationship between the dilution ratio of antibodies and the impedance changes caused by the immunoreaction (n=3, error bar represented R.S.D.).

### 3.4 The detection of AFB<sub>1</sub>

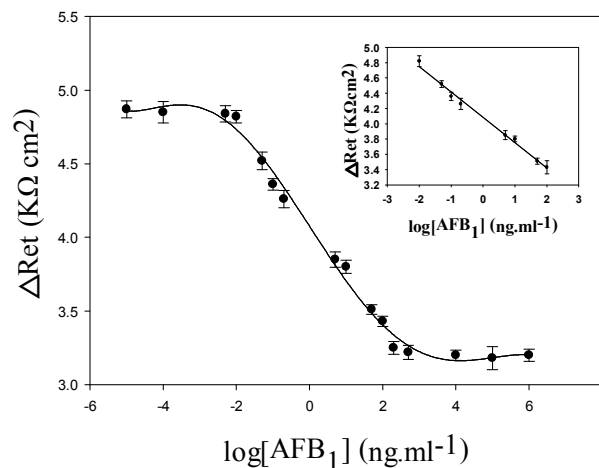


**Figure 7.** Impedance changes ( $\Delta R_{et}$ ) vs the logarithm of the AFB<sub>1</sub> concentration. All the measurements were carried out in 10 mM PBS (containing 0.1M KCl, 5 mM K<sub>4</sub>[Fe(CN)<sub>6</sub>]/K<sub>3</sub>[Fe(CN)<sub>6</sub>], pH 7.4) and the data were recorded in the frequency range from 0.1 Hz to 10 kHz. Inset: Linear relationship between the impedance changes ( $\Delta R_{et}$ ) and the logarithm of the different concentration of the AFB<sub>1</sub>. Error bars are the standard deviation of the mean n=3.  $r^2=0.9919$ . (n=3, error bar represented R.S.D.).



The electrochemical impedance immunosensor was applied to the detection of AFB<sub>1</sub> in samples to test its performance. Figure 7 illuminates the impedance changes ( $\Delta\text{Ret}$ ) responses to the specific immunointeraction on the sensing interface plotted versus the logarithm value of concentration of AFB<sub>1</sub>. The Ret decreased clearly with the increase of the concentration of AFB<sub>1</sub>, revealing the interactions between antibodies and antigens took place corresponding linearly to AFB<sub>1</sub>. A linear relation between the relative responses of the electron-transfer resistance and the logarithmic value of concentrations was observed in the range from 0.08 ng mL<sup>-1</sup> to 100.0 ng mL<sup>-1</sup>. And the response equation was shown as  $\Delta\text{Ret} (\text{K}\Omega \text{ cm}^2) = 4.09 - 0.332 \log C (\text{ng mL}^{-1})$  and a correlation coefficient was 0.9919 ( $n = 6$ ) ( $S/N=3$ ) (The inset in Figure 7). The detection limit (three times the signal to noise ratio) of the immunosensor was about 0.05 ng mL<sup>-1</sup>.

### 3.5 Reproducibility and Recovery of the modified electrodes

To investigate the immunoassay reproducibility of the sensor fabricated with the label-free method, the various concentrations of AFB<sub>1</sub> in the linear detection range were determined with the same electrode or different electrodes. The maximum relative standard deviations were 9.4% ( $n = 6$ ) for intraassay and 10.8% ( $n = 6$ ) for interassay.

To demonstrate the applicability and reliability of the immunosensor prepared using the present procedure, the recovery experiment of different AFB<sub>1</sub> concentration was performed. As seen in Table 1, recovery in the range of 88.0–112% with the relative standard derivation of 5.2–9.6% was achieved with all the measurements carried out four times.

**Table 1** Recovery studies of rice samples using immunoassay for AFB<sub>1</sub>

Sample NO.	Added AFB <sub>1</sub> (ng mL <sup>-1</sup> )	Found AFB <sub>1</sub> <sup>a</sup> (ng mL <sup>-1</sup> )	Recovery (%) <sup>a</sup>	RSD (%) <sup>a</sup>
1	0	0	/	/
2	2.5	2.2	88.0	5.9
3	12.5	11.4	91.2	9.0
4	50	52.2	104	7.5
5	100	99.0	99.0	8.8

<sup>a</sup>Each of the samples was evaluated in triplicate tests, and each of the results in Table 1 is the average of three parallel experiments.

### 3.6 Control experiments

To evaluate the selectivity of the proposed immunoassay, control experiments were performed using the other aflatoxins (AFB<sub>2</sub>, AFM<sub>1</sub>, AFM<sub>2</sub>) for comparison with AFB<sub>1</sub>. These drugs belonged to the class of the aflatoxins and were dissolved in PBS (pH7.4). These different immunosensors were used to detect 50 ng mL<sup>-1</sup> AFB<sub>1</sub> separately, the alternation antigen using the same method. The results of the study showed that the Ab was relatively specific for AFB<sub>1</sub> with cross-reactivity of 11% for AFM<sub>1</sub>, of 10% for AFM<sub>2</sub>, and of 40% for AFB<sub>2</sub>. The experimental results obtained indicate that the proposed sensor has reasonable specificity to AFB<sub>1</sub> as applied to the selective determination of the target analytes.

### 3.7 Agricultural sample analysis

The feasibility of the newly developed label-free immunoassay for possible applications was investigated by analyzing the agricultural samples, such as mouldy rice, mouldy corn and groundnuts samples. The samples were collected and the extraction procedure was performed as described by the literature<sup>14</sup>. Table 2 lists the AFB<sub>1</sub>

level determination results and the relative deviations of the proposed label-free immunoassay method as compared with the conventional AFB<sub>1</sub> analysis method in foods, ELISA. As can be seen in Table 2, the results of both methods were in reasonable agreement, suggesting that there is no difference of significance between the two methods and using the label-free immunosensor for the determination of AFB<sub>1</sub> concentration in foods and agricultural products is feasible.

**Table 2.** The results of AFB<sub>1</sub> level determination for two methods—the studied one and the ELISA one.

Samples	mouldy rice extract	mouldy corn extract	Groundnuts extract
By the proposed method (ng mL <sup>-1</sup> )	25.1	52.3	8.60
By ELISA method (ng mL <sup>-1</sup> )	24.3	51.9	9.10
Relative deviation (%)	2.29	5.43	3.99

\* Each of the samples was evaluated in triplicate tests, and each of the results in Table 2 is the average of three parallel experiments

## 4 Conclusions

In this work, a novel label-free impedance immunosensor for the direct detection of AFB<sub>1</sub> in foodstuffs is described. Compared with the conventional detection methods, the immunoassay was simple to perform and had a high selectivity in the detection of AFB<sub>1</sub>, without any redox probe or enzyme labeling. The reliability and applicability of directly detecting the antibody-antigen interaction by EIS measurement were also demonstrated. The results of the immunoassay for AFB<sub>1</sub> in foods were satisfactory. As expected, the proposed immunoassay has a great potentiality to be a new alternative method for the detection of AFB<sub>1</sub> in foods and agricultural products.

## Acknowledgements

This work was supported by National Grand (2009ZX10004-312), NSFC (21025521, 21035001), CSIRT program, NSF from Hunan Province (10JJ7002) and General Administration of Quality Supervision, Inspection and Quarantine of the People's Republic of China (No.2007GYB146).

## Notes and references

- a State Key Laboratory of Chem/Biosensing and Chemometrics, Chemistry and Chemical Engineering College, Hunan University, Changsha 410082, China. E-mail: rgyu@hnu.edu.cn; Fax: +86- 731- 8882 2782*  
*b Zhuzhou Office of Food Safety Committee, Zhuzhou, Hunan 412007, China*
- J. H. Owino, O. A. Arotiba, N. Hendricks, E. A. Songa, N. Jahed, T. T. Waryo, R. F. Ngece, P. G. Baker and E. I. Iwuoha, *Sensors*, 2008, 8, 8262.
  - M. S. Nasir and M. E. Jolley, *J. Agric. Food Chem.*, 2002, 50, 3116.
  - J. Gilbert, *Nat. Toxins*, 1999, 7, 347.
  - J. Gilbert and E. Anklam, *Trac-Trend Anal. Chem.*, 2002, 21, 468.
  - L. Lin, J. Zhang, P. Wang, Y. Wang and J. Chen, *J. Chromatogr. A*, 1998, 815, 3.
  - Y.-Y. Hu, P. Zheng, Z.-X. Zhang and Y.-Z. He, *J. Agric. Food Chem.*, 2006, 54, 4126.
  - I. A. Ahmed and R. K. Robinson, *J. Agric. Food Chem.*, 1998, 46, 580.

- 1  
2  
3  
4  
5  
6  
7  
8  
9  
10  
11  
12  
13  
14  
15  
16  
17  
18  
19  
20  
21  
22  
23  
24  
25  
26  
27  
28  
29  
30  
31  
32  
33  
34  
35  
36  
37  
38  
39  
40  
41  
42  
43  
44  
45  
46  
47  
48  
49  
50  
51  
52  
53  
54  
55  
56  
57  
58  
59  
60
- 8 M. Ventura, A. Gomez, I. Anaya, J. Diaz, F. Broto, M. Agut and L. Comellas, *J. Chromatogr. A*, 2004, 1048, 25.
- 9 L. E. Edinboro and H. T. Karnes, *J. Chromatogr. A*, 2005, 1083, 127.
- 10 H. Reinhard and B. Zimmerli, *J. Chromatogr. A*, 1999, 862, 147.
- 11 C. Cavaliere, P. Foglia, C. Guarino, M. Nazzari, R. Samperi and A. Laganà, *Anal. Chim. Acta*, 2007, 596, 141.
- 12 C. M. Maragos and J. I. Greer, *J. Agric. Food Chem.*, 1997, 45, 4337.
- 13 H. Cao, *Food Control*, 2011, 22, 43.
- 14 T. Yun, C. Xia, S. GuoLi and Y. RuQin, *Anal. Biochem.*, 2009, 387, 82.
- 15 A. Korde, U. Pandey, S. Banerjee, H. Sarma, S. Hajare, M. Venkatesh, A. Sharma and M. Pillai, *J. Agric. Food Chem.*, 2003, 51, 843.
- 16 S. Lipigorngoson, P. Limtrakul, M. Suttajit and T. Yoshizawa, *Food Addit. Contam.*, 2003, 20, 838.
- 17 M. Zayats, Y. Huang, R. Gill, C.-a. Ma and I. Willner, *J. Am. Chem. Soc.*, 2006, 128, 13666.
- 18 G. S. Bang, S. Cho and B.-G. Kim, *Biosens. Bioelectron.*, 2005, 21, 863.
- 19 A.-N. Kawde, M. C. Rodriguez, T. M. Lee and J. Wang, *Electrochem. Commun.*, 2005, 7, 537.
- 20 S. Zhang, F. Huang, B. Liu, J. Ding, X. Xu and J. Kong, *Talanta*, 2007, 71, 874.
- 21 S. Grant, F. Davis, K. A. Law, A. C. Barton, S. D. Collyer, S. P. Higson and T. D. Gibson, *Anal. Chim. Acta*, 2005, 537, 163.
- 22 X. Sun, H. Shi, H. Wang, L. Xiao and L. Li, *Ana. Letters*, 2010, 43, 533.
- 23 J.-D. Qiu, R.-P. Liang, R. Wang, L.-X. Fan, Y.-W. Chen and X.-H. Xia, *Biosens. Bioelectron.*, 2009, 25, 852.
- 24 A.-E. Radi, X. Munoz-Berbel, V. Lates and J.-L. Marty, *Biosens. Bioelectron.*, 2009, 24, 1888.
- 25 K. C. Grabar, R. G. Freeman, M. B. Hommer and M. J. Natan, *Anal. Chem.*, 1995, 67, 735.
- 26 Z.-S. Wu, M.-M. Guo, S.-B. Zhang, C.-R. Chen, J.-H. Jiang, G.-L. Shen and R.-Q. Yu, *Anal. Chem.*, 2007, 79, 2933.
- 27 L. Yang, Y. Li and G. F. Erf, *Anal. Chem.*, 2004, 76, 1107.
- 28 Z. Chen, J. Jiang, G. Shen and R. Yu, *Anal. Chim. Acta*, 2005, 553, 190.
- 29 M. Dijkstra, B. Kamp, J. Hoogvliet and W. Van Bennekom, *Anal. Chem.*, 2001, 73, 901.30 J. Randles, *J. Disc. Faraday Soc.*, 1947, 1, 1.